J Therm Anal Calorim (2011) 106:587–593
DOI 10.1007/s10973-011-1564-z

Rare-earth based OLEDs

TG-FTIR thermal stability investigation of tetrakis beta-diketonates complexes

Kelly C. Teixeira · Gabriela F. Moreira · Welber G. Quirino · Cristiano Legnani · Raigna A. Silva · Marco Cremona · Hermi F. Brito · Carlos A. Achete

CBRATEC7 Conference Special Issue

Abstract The improvement of operational lifetime and efficiency of organic light-emitting devices has stimulated many studies focused on the mechanisms responsible for their degradation. Such instabilities can be induced by several factors such as (i) current flow and heating, (ii) chemical reactions, (iii) self-conversion of the charge transporting molecules to cation, anion, and/or radical species. This work aims at investigating the thermal stability of rare-earth based tetrakis beta-diketonates complexes like $M[Eu(dbm)_4]$ ($M = Li^+$, $TMPip^+$, and $Morf^+$) through TG technique coupled with FTIR. Preliminary results show that $Li[Eu(dbm)_4]\cdot 4H_2O$ complex presents no degradation in its structure until 300 °C. However, evidences of rapid thermal degradation of the other two compounds have been found at temperatures lower than 100 °C, implying that these complexes could be degraded during the thermal deposition process at relatively high temperatures.

K. C. Teixeira · G. F. Moreira (✉) · W. G. Quirino · C. Legnani · R. A. Silva · M. Cremona · C. A. Achete
Divisão de Metrologia de Materiais, Inmetro, Duque de Caxias, RJ, Brazil
e-mail: gfmoreira@inmetro.gov.br

K. C. Teixeira · M. Cremona
Departamento de Física, Pontifícia Universidade Católica do Rio de Janeiro, PUC-Rio, Rio de Janeiro, RJ, Brazil

R. A. Silva
Instituto de Física, Universidade Federal de Uberlândia, Uberlândia, MG, Brazil

H. F. Brito
Departamento de Química Fundamental, Universidade de São Paulo, São Paulo, SP, Brazil

Keywords Rare-earth complexes · OLEDs · Thermal stability · TG-FTIR

Abbreviations

OLEDs	Organic light-emitting devices
RE	Rare-earth
RE^{3+}	Rare-earth ions
TG	Thermogravimetry
FTIR	Fourier Transform Infrared
DTG	Derivative thermogravimetry
IR	Infrared
λ	Wavenumber

Introduction

Over the last decade, organic light-emitting devices (OLEDs) have attracted great interest for their manifold applications in different areas, varying from white lighting, such as light bulbs replacement, to multicolor displays for televisions and cell phones. An organic LED (OLED) is a device composed of carbon-based films sandwiched between two charged electrodes, a metallic cathode and a transparent anode, usually glass. The OLEDs, generally, consist of a hole injection layer, a hole transporting layer, an emissive layer and an electron transporting layer. When voltage is applied to the OLED cell, the positive and negative charges injected from the electrodes recombine in the emissive organic layer, resulting in electroluminescent light. Several organic electroluminescent materials have been developed, with a main focus on fluorescent molecules and polymers [1, 2]. This kind of material, however, exhibits emission spectra with a typical width of 100–200 nm, which is not well suitable for display

applications. Pure red, green, and blue emissions are required, and in this context, rare-earth (RE)-based complexes are interesting candidates to be used for this purpose [3–5].

Due to the intra f–f transitions of rare-earth ions (RE^{3+}) and their unique ligand-mediated energy transfer mechanism, these ions present emission bands extremely sharp when electronic transitions occur, resulting in almost monochromatic and long-lifetime emission [6, 7]. Furthermore, once both singlet and triplet excitons are involved in the emission process and an efficient ligand-to-metal intramolecular singlet–triplet-rare earth ion energy transfer is operative, RE^{3+} can theoretically reach 100% quantum efficiency, which is four times higher than that of similar devices based on fluorescent materials.

In particular, RE^{3+} complexes with beta-diketonate ligands show intense photoluminescence [8] and electroluminescence [9, 10]. This is a consequence of the high absorption of the beta-diketonate species and its efficient energy transfer [11–13]. On the whole, the beta-diketonate-based OLEDs utilize neutral complexes which have three beta-diketonate ligands, with the general formula [RE(beta-diketonate)$_3$]. The insertion of a fourth beta-diketonate ligand and a counter-cation to achieve electric neutrality originates the tetrakis beta-diketonate complex, a system that has the first coordination sphere saturated. In this case, an improvement on light absorption by the antenna effect is expected [14].

Organic light-emitting devices based on RE^{3+} complexes are typically fabricated by vacuum vapor deposition technique, limiting the utilization for those complexes which do not present good thermal stability [15, 16]. In fact, the thin film deposition of these compounds requires their thermal heating up to temperatures of the order of 100–200 °C. Therefore, the investigation of the different thermal degradation processes which can occur in these complexes is fundamental to avoid their decomposition during the deposition, which can jeopardize the whole device.

The study of the decomposition of rare-earth complexes can be particularly difficult since their degradation can form various gaseous products and can present a number of decomposition steps in thermogravimetry (TG) experiments. The study of thermal stability by means of TG allows obtaining thermal decomposition data for further comprehension of the phenomenon and understanding the material performance. Coupling a TG instrument with a sophisticated gas analyzer such as an FTIR produces a powerful analytical technique that gives information with regard to the weight loss with respect to time and temperature, decomposition kinetics and functional group composition [17].

In this work, the investigation of thermal stability of novel tetrakis(beta-diketonates) complexes with general formula M[Eu(dbm)$_4$] (M = Li^+, $TMPip^+$, and $Morf^+$) through TG technique coupled with FTIR is presented and discussed.

Based on measurements, the TMPip[Eu(dbm)$_4$] (trimethypiperidinium tetrakis(dibenzoylmethanato)europate(III)) and Morf[Eu(dbm)4] (morpholinium tetrakis(dibenzoylmethanato)europate(III)) complexes show degradation starting from 70–90 °C, while the Li[Eu(dbm)$_4$]·4H_2O (lithium tetraaquatetrakis(dibenzoylmethanato)europate(III)) shows a better thermal stability without degradation until 300 °C. These results indicate that the tetrakis-beta-diketonates complexes with organic counter-cation ($TMPip^+$ and $Morf^+$) are very sensitive to temperature and cannot be used for thermally deposited organic layers involving temperatures higher than 100 °C.

Experimental details

Rare-earth based tetrakis (beta-diketonates) complexes like M[Eu(dbm)$_4$] (M = Li^+, $TMPip^+$ and $Morf^+$) were prepared by the method described in a previous work [18] and used without further purification and without pre-treatment before performing the TG experiments. Schematic draws of those complexes are shown in Fig. 1. The percentage wt/wt calculated of the water and chemical elements present in each complex is presented in Table 1 [18].

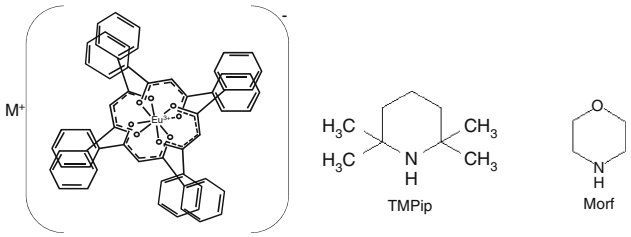

Fig. 1 Schematic structure of the rare-earth based tetrakis (beta-diketonates) complexes M[Eu(dbm)$_4$] (M = Li^+, $TMPip^+$, and $Morf^+$)

Table 1 Percentage wt/wt calculated of the water and chemical elements present in each complex

Chemical element	Percentage wt/wt calculated/%		
	Li[Eu(dbm)$_4$]·4H_2O	TMPip[Eu(dbm)$_4$]	Morf[Eu(dbm)$_4$]
Carbon	64.1	69.8	67.8
Hydrogen	4.7	5.4	4.8
Oxygen	17.1	10.8	12.71
Nitrogen	0.0	1.2	1.2
Europium	13.5	12.8	13.4
Lithium	0.6	0.0	0.0
Water	6.4	0.0	0.0

Thermogravimetry/derivative thermogravimetry curves and infrared spectra were obtained by a TG/DSC 1 Mettler-Toledo coupled to a FTIR Nicolet 6700 Thermo Scientific. Samples of 10 mg were loaded in Al_2O_3 pans and measured in the temperature range of 25 to 800 °C with a heating rate of 5 °C min^{-1} under nitrogen dynamic (50 mL min^{-1}). Infrared spectra with spatial resolution of 4 cm^{-1} were periodically collected during the entire run.

For the thin film deposition, Eu^{3+} complexes were deposited by thermal evaporation in tungsten crucibles with a controlled growth rate of about 0.1–0.3 nm s^{-1} under high vacuum and with a base pressure around 9×10^{-6} Torr. The photoluminescent spectra of the deposited thin films were recorded at room temperature with a Photon Technology International fluorescence spectrophotometer.

Results and discussion

Thermogravimetry (TG)

Thermal analyses of the complexes were carried out through TG/DTG techniques. Experimental results revealed that the thermal degradation of the three complexes occurred in multiple stages, following a complex mechanism with four or five decomposition stages, as can be seen in Fig. 2.

TG curve for $Li[Eu(dbm)_4]\cdot 4H_2O$ complex (Fig. 2b) presents four main stages of mass loss and two minor ones. At the first stage (up to 100 °C), there is about 8% of mass loss possibly corresponding to adsorbed water and weakly bound water. This inference comes from FTIR spectrum that shows an increase of relative intensities of bands assigned to vibrations of OH bonds (around 1500 and 3500 cm^{-1}) between 28 and 96 °C (Fig. 3a) and is also in accordance with water percentage wt/wt calculated (6.5%) for $Li[Eu(dbm)_4]\cdot 4H_2O$ complex (Table 1). Between 100 and 300 °C, the curve remains practically stable. At about 300 °C, a second event of mass loss begins. From this point, the weight loss is attributed to thermal degradation of the complex as indicated by the increase in relative intensity of the absorption band corresponding to C=O double bonds, between 2250 and 2500 cm^{-1} in FTIR spectra—Fig. 3b and c, and probably due to CO_2 emissions. According to DTG curve (Fig. 2b), the maximum degradation occurs at around 420 °C, with 43% of mass loss. The second event of thermal degradation, with 23% of total mass loss, occurs at around 540 °C. Finally, the last stage of degradation, corresponding to 8% mass loss, involves three smaller events starting, respectively, at around 660, 700, and 750 °C. Completed the analysis, a residual mass at about 18% was observed if compared to the initial mass of the sample.

For $TMPip[Eu(dbm)_4]$ and $Morf[Eu(dbm)_4]$ compounds (Fig. 2c, d), initial water loss is hardly observed; the second of them, for instance, presents only 2% of initial mass loss associated with adsorbed water. However, from 100 to 800 °C, a continuous degradation of both complexes through various stages of thermal decomposition was observed. This result is confirmed by the absorption spectra obtained from evolved gases, in which the continuous increase in CO_2 gas emission is evidenced, as before, by the increased relative intensity of C=O band between 2250

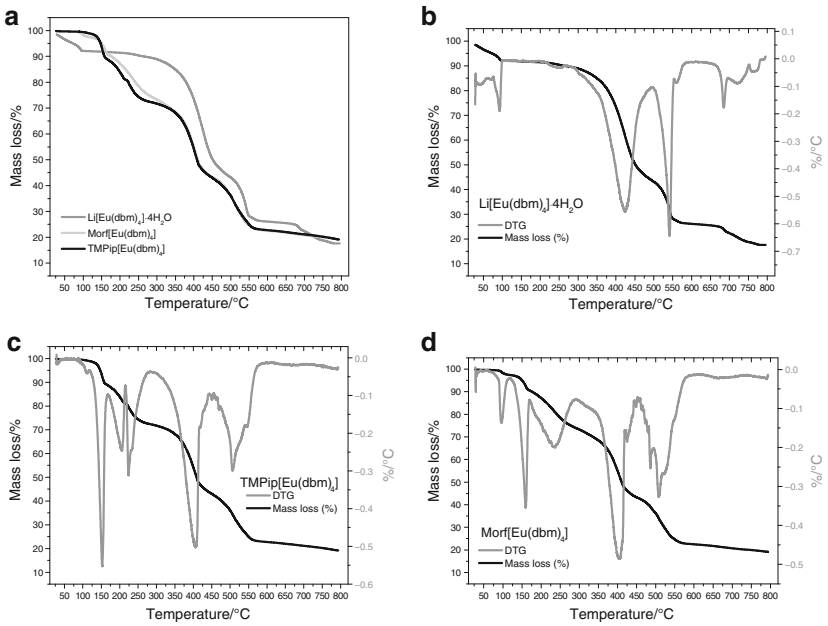

Fig. 2 TG/DTG curves for complexes obtained under dynamic atmospheres of N_2 (50 mL min^{-1}) in the temperature range of 25 to 800 °C with a heating rate of 5 °C min^{-1}: **a** TG curves of all complexes; **b** $Li[Eu(dbm)_4]\cdot 4H_2O$ complex; **c** $TMPip[Eu(dbm)_4]$ complex; **d** $Morf[Eu(dbm)_4]$ complex

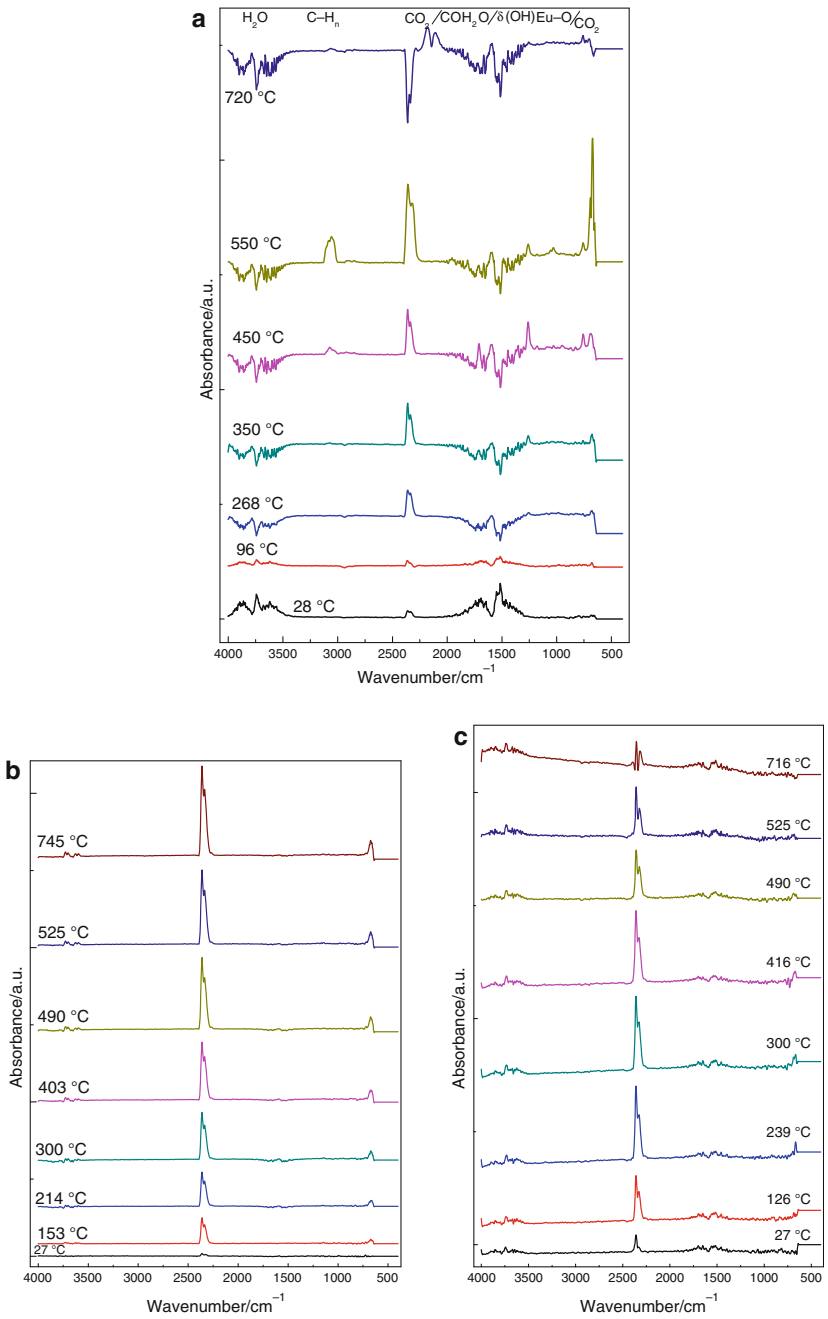

Fig. 3 IR absorption spectra for the complexes in the range of 650–4000 cm^{-1} and at different temperature of TG analysis: **a** $Li[Eu(dbm)_4]\cdot 4H_2O$; **b** $TMPip[Eu(dbm)_4]$; **c** $Morf[Eu(dbm)_4]$

and 2500 cm^{-1} (Fig. 3b, c). The similar thermal behavior confirms the low thermal stability of these compounds. In the TG/DTG curves, five events related to the thermal degradation of both materials have been observed.

Table 2 presents the initial temperature (T_i), the maximum temperature (T_{max}) and the final temperature (T_f) of degradation for each thermal event with its corresponding mass loss. The final residual mass of each sample at the end of the experiment is also reported. The $Morf[Eu(dbm)_4]$ complex ended up being slightly less stable, with lower initial temperatures of degradation. Probably, this lower degradation temperature is due to the presence of adsorbed water and oxygen in its structure, as shown in the FTIR spectra. In addition, in all the studied complexes, the first decomposition step corresponds to the loss of the coordinated water and/or CO_2 in the temperature range of 25–150 °C. Other decomposition steps, at 150–450 °C temperature range, involve the removal of some terminal and/or integral parts in all ligands [19].

The final degradation step (centered around 500–600 °C) involves removal of ions. The high percentage of intact residue in all complexes—about 18 to 19% of original mass—may be possibly associated with the stability of the coordination sphere around europium atom with other

Table 2 Initial temperature (T_i), maximum temperature (T_{max}), final temperature (T_f) of degradation for each event and its corresponding mass loss and the final residual mass for all complexes studied

Decomposition events	$Li[Eu(dbm)_4]\cdot 4H_2O$				$TMPip[Eu(dbm)_4]$				$Morf[Eu(dbm)_4]$			
	T_i/°C	T_{max}/°C	T_f/°C	Mass loss/%	T_i/°C	T_{max}/°C	T_f/°C	Mass loss/%	T_i/°C	T_{max}/°C	T_f/°C	Mass loss/%
First	28		100	8	92	150	157	10	73	95	118	2
Second	300	420	460	43	157	205	215	8	118	159	168	7
Third	460	540	600	23	215	224	283	8	168	235	265	15
Fourth	660		780	8	283	405	415	26	265	405	415	30
Fifth					415	506	600	25	415	506	600	25
Residual mass at 800 °C/%	18				19				19			

residues, as indicated for europium percentage wt/wt calculated for different complexes (Table 1).

FTIR analysis

Figure 3 shows FTIR absorption spectra for all the three complexes and at different temperatures of TG analysis. For each time (or temperature), the measurement of the IR absorption of the evolved gases was performed, allowing the identification of the type of the chemical bonds or functional groups present in these gases.

According to Fig. 2 (TG/DTG), the maxima of the generated volatile products can be found in the corresponding spectra of Fig. 3. These maxima are coincident with the maxima of absorbance observed in the scale of relative time of: (a) $Li[Eu(dbm)_4]\cdot 4H_2O$ complex—0, 882, 2938, 3960 s (first step at around 28, 96, 268, and 350 °C, respectively), 5100 s (second step, at around 450 °C) and 6240 s (third step, at around 550 °C); (b) $TMPip[Eu(dbm)_4]$ complex—0, 1560 s (first step at around 25 and 153 °C, respectively), 2580 s (third step, at around 239 °C), 3300, 4500 s (fourth step at around 300 and 403 °C, respectively) and 5580, 6000 s (fifth step at around 490 and 525 °C, respectively); (c) $Morf[Eu(dbm)_4]$ complex—0 s (first step at around 27 °C), 1680 s (second step at around 157 °C), 25800 s (third step at around 239 °C), 3300 and 4680 s (fourth step, at around 300 and 416 °C, respectively), 5580 and 6000 s (fifth step at around 490 and 525 °C, respectively).

Analysis of the different IR spectra obtained in Fig. 3a for the $Li[Eu(dbm)_4]\cdot 4H_2O$ complex reveals the existence of absorption bands in the range of 3130–2990 cm^{-1} corresponding to the C–H bonds and in the range of 2400–2230 cm^{-1} due to CO_2 concentration in the system. At around 450 °C, it is possible to observe the appearance of two peaks centered at about 1260 [20] and 757 cm^{-1} [21]. These peaks can be related to the deformation mode and metal–oxygen stretching mode for the OH and Eu^{+3}, respectively. Above 550 °C, a decrease in the band intensities and the appearance of two strong bands in the range of 2264–2034 cm^{-1} suggest the cracking of CO bonds present in the complex. Up to 700 °C, the IR spectrum shows the formation of higher amounts of CO_2 and CO. This step could be related to the decomposition of mineral matter. On the other hand, downward peaks, occurring in the spectra, correspond to the decrease in free water concentration—due to poor purge—initially present in the system.

Figure 3b shows absorption spectra corresponding to the gases obtained for the $TMPip[Eu(dbm)_4]$ complex. The analysis of these spectra shows the existence of many common bands, with the main differences in the 4000–650 cm^{-1} range. A noticeable increase of the peak at

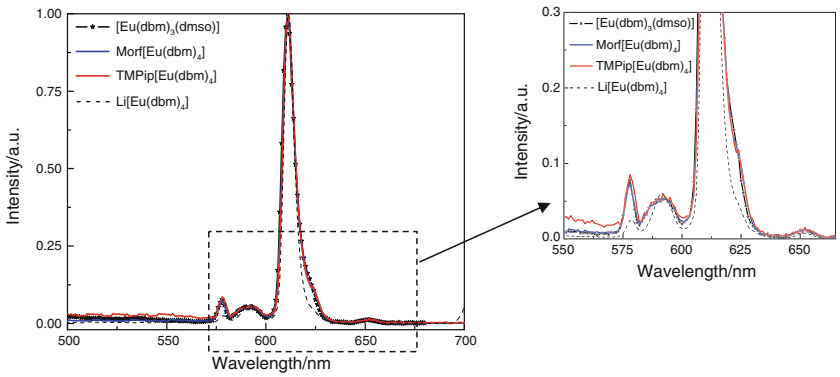

Fig. 4 Comparison between the photoluminescence spectra of thin films of the three Eu-based tetrakis-beta-diketonate complexes with that of the tris-beta-diketonate $Eu(dbm)_3(dmso)$ complex. The detail shows a region where the differences are more evident

2360 cm^{-1}, corresponding to CO_2, can be observed, as well as the appearance of absorption bands in the region of 672 and 3750–3550 cm^{-1} corresponding to the water bending mode [20] and OH and NH functional groups stretching modes which are present in the complex. Furthermore, the absorption bands present in the IR spectrum at around 28 °C corresponding to the first decomposition step are similar to those present at 745 °C—for the last decomposition stage. This result indicates that TMPip[Eu(dbm)$_4$] complex is unstable just above room temperature.

Finally, Fig. 3c shows the IR spectra corresponding to all decomposition stages observed in the Morf[Eu(dbm)$_4$] complex. These spectra show the continuous formation of free water and water loosely bound to complex and CO_2 in the regions of 3750–3550 and 2400–2230 cm^{-1}, respectively. In this compound, the shape and the energy of the absorption bands is close to that of TMPip[Eu(dbm)$_4$] complex. In addition, at about 400 °C, there was an increase of the emission coupled to absorption bands in the IR spectra. This emission suggests that this compound is chemiluminescent on oxidation, with reasonable efficiency. The chemiluminescent process can thus be due to excited carbonyl fragments emitters [22].

The lower thermal stability of Morf[Eu(dbm)$_4$] and TMPip[Eu(dbm)$_4$] complexes can be also observed when thin films of these materials are thermally deposited onto quartz substrates in high vacuum environment. When excited with $\lambda = 360$ nm, their photoluminescence spectra show the typical sharp lines of the Eu ion transitions (Fig. 4).

A thorough analysis, however, reveals that the Li[Eu(dbm)$_4$]·4H_2O spectrum (dashed line in Fig. 4) does not match those of the Morf and TMPip complexes very well (solid lines in Fig. 4). On the other hand, these spectra overlap almost perfectly with the spectrum of the *tris*-beta-diketone Eu(dbm)$_3$(dmso) complex (where dmso = methyl sulfoxide), dashed-star line in Fig. 4. This can be an indication that during the thermal deposition, the Morf and TMPip tetrakis complexes undergo a thermal degradation resulting in the more stable tris-species. This does not happen for the Li[Eu(dbm)$_4$]·4H_2O, which is thermally more stable, as the TG-FTIR measurement indicates.

Conclusions

The TG-FTIR results suggest that Li[Eu(dbm)$_4$].4H_2O complex is thermally more stable than the other two tetrakis-beta-diketonate complexes since it shows no degradation events until ~300 °C. This is an indication that the metallic Li^+ counter-cation is strongly linked to the rare-earth based complex, allowing the utilization of this compound in OLEDs fabrication. Conversely, Morf[Eu(dbm)$_4$] and TMPip[Eu(dbm)$_4$] complexes present a lower thermal stability, evidenced by significant mass loss at low temperatures (in the range of 100–200 °C) and by the increase of the bands related CO_2 emissions present in their FTIR spectra. One may conclude that the counter-cations $Morf^+$ and $TMPip^+$ are weakly linked to the rare-earth complex and would possibly degrade during the thermal deposition process at relatively high temperatures. The preliminary photoluminescence measurement seems to indicate that the degradation can lead to change the tetrakis-species in the more stable tris.

Acknowledgements The authors would like to acknowledge the financial support granted by the following Brazilian agencies: FINEP, CAPES, CNPq, and FAPERJ.

References

1. Xu F, Wang C, Yang L, Yin S, Wedel A, Janietz S, Krueger H, Hua Y. PPV-derivatives containing phenothiazine and alkyloxy-substituted oxadiazole/phenyl units for OLED. Synth Met. 2005; 152:221–4.
2. Li H, Zhang F, Wang Y, Zheng D. Synthesis and characterization of tris-(8-hydroxyquinoline)aluminum. Mate Sci Eng B. 2003; 100:40–6.
3. Kido J, Okamoto Y. Organo lanthanide metal complexes for electroluminescent. Mater Chem Rev. 2002;102(6):2357–68.
4. Silva CR, Li F, Huang C, Zheng Z. Europium β-diketonates for red-emitting electroluminescent devices. Thin Solid Films. 2008; 517:957–62.
5. Guedes MA, Paolini TB, Felinto MCFC, Kai J, Nunes LAO, Malta OL, Brito HF. Synthesis, characterization and spectroscopic investigation of new tetrakis(acetylacetonato)thulate(III) complexes containing alkaline metals as countercations. J Lumin. 2011;131:99–103.
6. Xua H, Yinc K, Huang W. Synthesis, photophysical and electroluminescent properties of a novel bright light-emitting Eu^{3+} complex based on a fluorene-containing bidentate aryl phosphine oxide. Synth Met. 2010;160:2197–202.
7. Araujo AAS, Brito HF, Malta OL, Matos JR, Teotonio EES, Storpirtis S, Izumi CMS. Synthesis and photophysical study of highly luminescent coordination compounds of rare earth ions with thenoyltrifluoroacetonate and AZT. J Inorg Biochem. 2002; 88:87.
8. Brito HF, Teotonio EES, Fett GM, Faustino WM, Sá GF, Felinto MCFC, Santos RHA. Evaluation of intramolecular energy transfer process in the lanthanide(III) bis- and tris-(TTA) complexes: photoluminescent and triboluminescent behavior. J Lumin. 2008; 128:190–8.
9. Quirino WG, Legnani C, Dos Santos R, Teixeira K, Cremona M, Guedes MA, Brito HF. Electroluminescent devices based on rare-earth tetrakis beta-diketonate complexes. Thin Solid Films. 2008; 517:1096–100.
10. Chen Z, Ding F, Hao F, Bian Z, Ding B, Zhu Y, Chen F, Huang C. A highly efficient OLED based on terbium complexes. Org Electron. 2009;10:939–47.
11. Yang C, Luo J, Ma J, Liang L, Lu M. Highly quantum efficiency trinuclear Eu^{3+} complex based on tris-diketonate ligand. Inorg Chem Commun. 2011;14:61–3.

12. Wua J, Li H, Xu Q, Zhu Y, Tao Y, Li H, Zheng Y, Zuo J, You X. Synthesis and photoluminescent properties of series ternary lanthanide (Eu(III), Sm(III), Nd(III), Er(III), Yb(III)) complexes containing 4,4,4-trifluoro-1-(2-naphthyl)-1,3-butanedionate and carbazole-functionalized ligand. Inorg Chim Acta. 2010;363:2394–400.
13. Sá GF, Malta OL, Donegá CM, Simas AM, Longo RL, Santa-Cruz PA, Silva EF Jr. Spectroscopic properties and design of highly luminescent lanthanide coordination complexes. Coord Chem Rev. 2000;196:165–95.
14. Brito HF, Malta OL, Felinto MCFC, Teotonio EES. The chemistry of metal enolates. In: Zabicky J, editor. Luminescence phenomena involving metal enolates. 1st ed. England: Wiley; 2009. p. 131–84.
15. Yan CH, Hu HH, Xu CJ, Zhu W, Zhang M, Bu XR. Synthesis and characterization of photoluminescent terbium-containing polymer precursors. J Photochem Photobiol A. 2009;204:19–24.
16. Arnautova S, Nechvolodova E, Lomakin S, Shchegolikhin A. Photo- and thermal-oxidative stability of novel material for photovoltaics: MEH-PPV/TNF blends. Renew Energy. 2008;33:259–61.
17. Chattopadhyay DK, Webster DC. Thermal stability and flame retardancy of polyurethanes. Prog Polym Sci. 2009;34:1068–133.
18. Guedes MA, de Doutoramento Tese. Comportamento fotoluminescente dos ânions complexos tetrakis(-dicetonatos) de Íons terras raras—Eu^{3+}, Gd^{3+}, Tb^{3+} e Tm^{3+}. São Paulo: Instituto de Química; 2008.
19. El-Ayaan U, El-Metwally NM, Youssef MM, El Bialy SAA. Perchlorate mixed-ligand copper(II) complexes of β-diketone and ethylene diamine derivatives: thermal, spectroscopic and biochemical studies. Spectrochim Acta A. 2007;68:1278–86.
20. Nakamoto K. Infrared and Raman spectra of inorganic and coordination compounds. 3rd ed. New York: Wiley; 1978.
21. Tsaryuk V, Zolin V, Legendziewicz J, Szostak R, Sokolnicki J. Effect of ligand radicals on vibrational IR, Raman and vibronic spectra of europium beta-diketonates. Spectrochim Acta A. 2005;61:185–91.
22. Elbanowski M, Staninski K, Kaczmarek M. The nature of the emitters in Eu(II)/(III)-coronand-H_2O_2 chemiluminescent systems. Spectrochim Acta A. 1998;54:2223–8.